Renewable Energy 145 (2020) 1014–1019

Contents lists available at ScienceDirect

Renewable Energy

journal homepage: www.elsevier.com/locate/renene

Ethyl esters biodiesel production from *Spirulina sp.* and *Nannochloropsis oculata* microalgal lipids over alumina-calcium oxide catalyst

Berk Turkkul, Ozgun Deliismail, Erol Seker*

Izmir Institute of Technology, Chemical Engineering Department, Gulbahce Campus, Urla, Izmir, 35430, Turkey

ARTICLE INFO

Article history:
Received 10 January 2019
Received in revised form
10 May 2019
Accepted 17 June 2019
Available online 20 June 2019

Keywords:
Ethyl ester biodiesel
Nannochloropsis oculata
Spirulina sp.
Heterogeneous catalyst
Sol gel

ABSTRACT

In this study, we present the ethyl esters biodiesel production from *Nannochloropsis oculata* and *Spirulina sp.* microalgal lipids on 60 wt% CaO on Al_2O_3 catalyst at 50 °C and 1.0 atm. The activity of the catalyst was studied as a function of ethanol:lipid molar ratios, catalyst amounts and reaction times. It was found that 6 wt% of the lipids as catalyst amount resulted in 59% biodiesel yield in 30 min at 12 of ethanol:lipid molar ratio whereas 90–99% biodiesel yield was obtained at 24 and 48 of ethanol:lipid molar ratios. In order to achieve 90–99% yields, the basic strength was found to be weak and to be in the form of bicarbonate, whereas high basicity was not necessary. Besides, pure CaO and Al_2O_3 were not active under the same reaction conditions. We found that the glycerolysis of triacylglyceride occurred in series with the reverse of the transesterification of the triacylglyceride when the catalyst amount was 6 wt% of the lipids and the ethanol:lipid molar ratio was 24 and 48 and the reaction time was 60 min.

1. Introduction

The fossils fuels and their derivatives have been the main energy sources in transportation, industrial and residential operations. Unfortunately, their usages have increased air pollutant emissions, such as greenhouse gases, for decades [1,2]. The major contributor is the transportation sector; for instance 28% of total CO_2 emission and ~84% of the transportation related CO_2 emission comes from the road transportation [3]. On the other hand, biofuels, which are CO_2 neutral fuels, are viable choices to replace fossil fuels but their most significant drawback was the operating cost of their production. For instance, ~80% of the total cost in the biodiesel production using oil crops was related to its operating cost. Besides, the usage of the oil crops for fuels production was not desirable due to increasing demand of oil crops for human consumptions [4]. Therefore, an alternative oil source could be lipid containing aquabiomass, such as microalgae or macroalgae.

The usage of microalgae as compared to macroalgae has many advantages. For instance, microalgae have high growth rates; e.g. doubling in 24 h [5]; 15–300 times more oil production using microalgae than traditional oil crops on an area basis could be possible [6]; microalgal lipid contents could be adjusted with the change of growth medium composition [7]; multiple times harvesting a year are possible [8]; salty or waste water and atmospheric carbon dioxide as the carbon source are used in growing microalgae; and they are non-toxic and highly biodegradable [8].

Biodiesel can be produced with the transesterification and/or esterification of variety of microalgal/macroalgal lipids and an alcohol in the presence of a catalyst. In general, methanol as the alcohol and sulfuric acid or sodium hydroxide as the homogeneous catalyst has been used because of their high activities at low temperatures and 1.0 atm. For instance, Miao and Wu [9] reported the production of methyl esters biodiesel from heterotrophically grown *Chlorella protothecoides* microalgae using sulfuric acid and methanol at 30 °C whereas Li et al. [10] showed that 98.2% of *Chlorella protothecoides* microalgae could be converted to biodiesel using an immobilized lipase in 12 h. In addition, Hossain et al. [11] showed that biodiesel could be produced from the lipids of macroalgae species, *Oedigonium* and *Spirogyra,* and methanol using sodium hydroxide as the catalyst. In contrast, there are few studies and some patents on the methyl ester biodiesel production from microalgal lipids and methanol over heterogeneous catalysts in the literature. For instance, Umdu et al. [12] was the first to report highly active alumina supported calcium oxide and magnesium oxide catalysts made with a sol-gel method in the

* Corresponding author.
E-mail address: erolseker@iyte.edu.tr (E. Seker).

https://doi.org/10.1016/j.renene.2019.06.093
0960-1481/

transesterification of *Nannochloropsis oculata* at 50 °C and 1.0 atm. Carrero et al. [13] showed that 25% of the highest biodiesel yield was obtained in the esterification of *N. gaditana* microalgal lipid with methanol over H-Beta zeolite, ZSM-5, Beta, and H-ZSM-5 zeolites at 115 °C in 4.0 h. Teo et al. [14] reported that 92% of biodiesel yield was achieved using calcium methoxide catalyst and methanol in the transesterification of *Nannochloropsis oculata* microalgal oil at 60 °C in 30–240 min. Similarly, Carrero et al. [15] observed 94% of the highest biodiesel yield at 100 °C in 4.0 h from *N. gaditana* microalga in the esterification/transesterification using methanol over Amberlyst-15, CT-269, CT- 275, KSF clay and silica-alumina catalysts. But they reported very low reusability of the ion-exchanged resin catalysts. Recently, Guldhe et al. [16] reported that ~98% of *Scenedesmus obliquus* microalgal lipid was converted to methyl ester biodiesel over chromium-aluminum mixed oxide catalyst, prepared with a precipitation method, in the presence of methanol in 4.0 h at 80 °C.

The use of ethanol instead of methanol in the production of biodiesel seems to be a better alternative because ethanol is produced from biological sources and also, improves cold temperature issues, such as cloud point, of the biodiesel [17]. There are few studies on the use of ethanol and vegetable oils over homogeneous and heterogeneous catalysts in the production of ethyl esters biodiesel [18–20]. However, to the best of our knowledge, there are no studies on the production of ethyl esters biodiesel from microalgal lipids and ethanol over heterogeneous catalysts at 50 °C and 1.0 atm in the literature.

In this study, ethyl esters biodiesel production from *Spirulina sp.* (preferred due to commercial availability in large quantities, [4]) and *Nannochloropsis oculata* (*N.oculata*) marine microalgae (preferred due to its high fatty acid content, [4–6]) over an alumina-calcium oxide catalyst was studied as a function of ethanol:lipid molar ratios, the amount of the catalyst and the reaction time at 50 °C and 1.0 atm.

2. Material and methods

2.1. Catalyst preparation

Alumina-calcium oxide catalyst, 60 wt% CaO on Al_2O_3, was synthesized using a modified single step sol–gel method [12,21,22]. The single step sol-gel preparation method and the drying procedure were the same as the procedures given by Yalman [22] but the calcination temperature and the calcination time used in this study was 700 °C and 6.0 h, respectively. Finally, the calcined catalyst was ground and sieved to less than 325 mesh sizes prior to be used in the activity measurements.

2.2. Algal lipid extraction and ethyl ester biodiesel production

Freeze dried *Spirulina sp.* marine microalgae powder, grown organically and free of additives and irradiation, was purchased from Optimally Organic Inc. Also, *N. oculata* marine microalgal paste, grown in a growth medium and harvested with the method given in the literature [23], was obtained from Prof. Dr. Durmaz of Ege University. The paste was dried at 60 °C under vacuum of 100 mbar for 12 h. Then, microalgal lipids from dried *Spirulina sp.* and *N. oculata* marine microalgae powders were extracted with hexane in a Soxhlet extractor operated at 80 °C for 10–24 h using a similar procedure given by Miao and Wu [9]. The extraction procedure used in this study was the partial extraction because hexane was non-polar solvent; thus, eliminating the extraction of non-lipid and polar-lipid compounds [24–26]. After the extraction, the excess hexane was evaporated using a rotary evaporator at 50 °C and 100 mbar to obtain the microalgal lipid.

2.3. Catalyst activity and characterization

In our recent study [22], similar 60 wt% CaO on Al_2O_3 catalyst whose the calcination temperature was different was used in the transesterification of canola oil with ethanol and we found that ~100% ethyl ester biodiesel yield was obtained in less than 1.0 h under the reaction condition of 9:1 ethanol:canola oil molar ratio and 6.0 wt% of the oil as the catalyst amount at 50 °C. Therefore, 60 wt% CaO on Al_2O_3 catalyst calcined at 700 °C was used in the production of the ethyl esters biodiesel from *Spirulina sp.* and *N. oculata* microalgal lipids and ethanol in a batch reactor at 50 °C and 1.0 atm under the following reaction conditions: 12:1.0, 24:1.0 and 48:1.0 of ethanol:lipid molar ratios; 6.0 wt%, 12 wt% and 18 wt% of the lipid as the catalyst amounts; and 30 min, 60 min and 120 min of the reaction times.

All the reaction conditions in the production of ethyl esters biodiesel from microalgal lipids over the catalyst resulted in a single liquid phase formation since ethanol:oil molar ratios were in excess of the stoichiometric molar ratio. In our previous studies [21,22], we developed a procedure in our lab to separate the single liquid phase into biodiesel and glycerol rich phases (details are given in Supplementary Materials). This separation procedure resulted in the biodiesel rich phase, containing biodiesel amount greater than 98 wt% as determined by GC analyses (a GC chromatogram is also given in Supplementary Material). The analyses were done using Agilent 6890 N Ga Chromatograph equipped with a FID detector and a DB-WAX 122–7032 column with a 60 m of column length, 0.25 mm of column diameter and 0.25 μm of film thickness. The separation in the column was achieved using an isothermal analysis method: The column was at 225 °C and for injection port and detector, 250 °C was used. Helium flow and split ratio were set at 32 cm/s and 150, respectively. Biodiesel yield was calculated using the following equation:

$$\text{Biodiesel yield (wt\%)} = \frac{\text{amount of ethyl ester biodiesel (g) in upper phase}}{\text{initial amount of microalgal lipid (g)}} \text{x100}$$

Crystalline phases present in the catalysts were determined by X-ray diffraction technique (Philips X'pert Pro XRD, operated at 40 kV and 45 mA) and also average crystallite sizes were calculated from the peak broadening of the diffraction peaks using Scherrer equation given below.

$$d = \frac{K\,\lambda}{(B\,Cos\theta)}$$

where d was the average crystallite size, K was Scherrer constant (~0.9), λ was the wavelength of the X-ray (λ = 0.15406 nm), B was the peak broadening of a diffraction peak found using the full width at half maximum (given in radian) of the peak and θ was the main diffraction angle of the peak given in degree [27].

The basicity and basic strength of all the catalysts were determined using FTIR with carbon dioxide as the probe molecule. The amount of irreversibly adsorbed CO_2 gave the total amount of basic sites on solid surfaces and also, its absorption band wavenumber was the strength of the basic site [28].

3. Results and discussion

3.1. Crystalline phases and basicities of the catalysts

As seen in Fig. 1, the analysis of XRD pattern of 60 wt% CaO/Al_2O_3 catalyst using standard diffraction reference patterns on X'Pert HighScore Plus software (PANalytic B.V.) showed that the

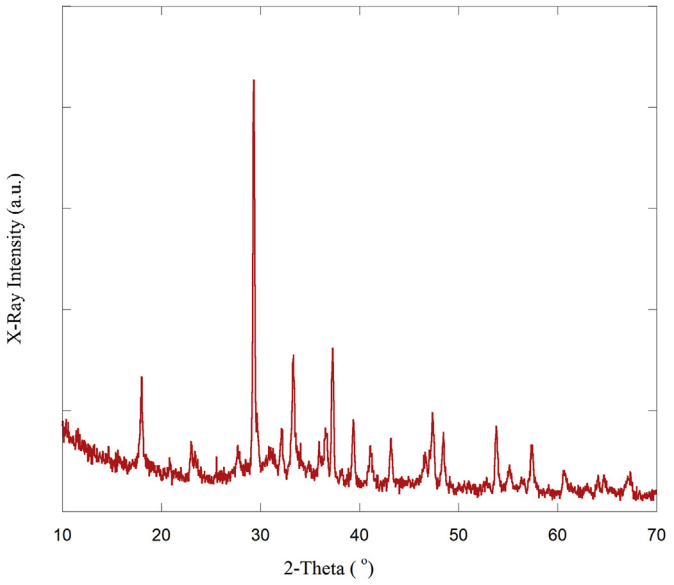

Fig. 1. XRD of 60%CaO/Al_2O_3 calcined at 700 °C.

diffraction patterns of 60 wt% CaO/Al_2O_3 catalyst corresponded to CaO, $Ca(OH)_2$, $CaCO_3$ and Al_2O_3 crystalline phases and also the hydrated form of the mixture of these crystalline phases, such as $2CaO.Al_2O_3.8H_2O$ and $3CaO.Al_2O_3.3CaCO_3.3H_2O$ [29]. The diffraction angles observed on 60 wt% CaO/Al_2O_3 catalyst, their matching crystalline phases and their matched standard reference card numbers were listed in Table 1. The average crystallite sizes of CaO, $Ca(OH)_2$ and, $CaCO_3$ using non-overlapping peaks was calculated to be 43.9 nm, 27.4 nm and 39.59 nm, respectively whereas it was not possible to calculate the crystallite sizes for Al_2O_3 and the hydrated forms of the mixed crystalline phases because of their diffraction peaks overlapping with other peaks. In addition, the crystalline phases and crystallite sizes of commercial pure CaO, $CaCO_3$ and $Ca(OH)_2$ and pure Al_2O_3 made in this study using the same sol-gel method were determined using the XRD and their patterns are given in the supplementary materials (Figs. S3–S4). The analyses of XRD patterns using standard diffraction reference patterns on X'Pert HighScore Plus software showed that pure CaO had calcium oxide and also, $Ca(OH)_2$ (due to adsorption of moisture from air during XRD measurement) crystalline phases and its average crystallite size was 77 nm. Pure Al_2O_3 contained gamma alumina crystalline phase and its average crystallite size was 82 nm.

As seen in Table 2, the total basicity of 60 wt% CaO/Al_2O_3 was determined to be 41 μmol CO_2/g of catalyst whereas the basicities of pure Al_2O_3 and pure CaO were 47.1 and 192.6 μmol CO_2/g of catalyst, respectively. In other words, the basicity of pure alumina was ~1.15 times higher than that of 60 wt% CaO/Al_2O_3 and also the basicity of pure CaO was 4.7 times higher that of 60 wt% CaO/Al_2O_3. Thus, one may expect to obtain higher biodiesel formation on the catalysts having high basicities but interestingly, we found that there was no conversion of microalgal lipid to ethyl esters on pure alumina and pure CaO catalysts. In contrast, the conversion to ethyl esters biodiesel on 60 wt% CaO/Al_2O_3 catalyst that had lower basicity was higher than 58% which depended on the reaction conditions. This indicated that the basicity alone could not explain high microalgal lipid conversion over 60 wt% CaO/Al_2O_3 catalyst. This high conversion could be related to varying basic strengths on 60 wt% CaO/Al_2O_3, pure CaO and pure Al_2O_3 catalysts.

The absorption band wavenumber of CO_2 on the catalysts is related to the strengths of the basic sites [28]. As seen in Table 2, on pure CaO, we observed two weak CO_2 absorption bands at 1074 and 1794 cm^{-1} and a strong absorption band centered at 1454 cm^{-1} with a band splitting at 1424 and 1484 cm^{-1} and this strong band had a weak shoulder at 1653 cm^{-1}. In addition, there was a weak band at 2564 cm^{-1}. These observed bands were in parallel with the studies on IR bands observed for CO_2 adsorbed on pure CaO in the literature. For instance, Gurene et al. [30] assigned the bands at 1630, 1460 and 1213 cm^{-1} to bicarbonate species and also, the bands at 1560, 1390, and 1069 cm^{-1} were assigned to unidentate carbonate on pure CaO surface. Also, Zaki et al. [31] reported similar IR absorption bands of CO_2 adsorbed on pure CaO obtained by calcining calcium hydroxide at 700 °C for 3 h. Thus, we assigned the band at 1074 cm^{-1}, the band with the splitting at 1424 and 1484 cm^{-1}, that had the weak shoulder at 1653 cm^{-1}, to the stretching band of C—O bond and symmetric/asymmetric stretching bands of O—C—O bonds of unidentate carbonate. In addition to these bands, the weak bands at 1794 cm^{-1} and 2564 cm^{-1} were assigned to the bridging carbonate species and to linearly adsorbed CO_2 at a cation site, respectively. These results showed that the unidentate carbonate species dominated on pure CaO. However, on 60%CaO/Al_2O_3 catalyst, we observed weak bands located at 1266 and 1798 cm^{-1} and a strong band at 1432 cm^{-1} with shoulders at 1333 and 1635 cm^{-1}. Besides, the band 1432 cm^{-1} did not have the band splitting. Thus, the band at 1266 cm^{-1} was assigned to C—OH bending and bands at 1333, 1432 and 1635 cm^{-1} were assigned to the symmetric and asymmetric stretching of O—C—O of bicarbonate species and the band at 1798 cm^{-1} was assigned to the stretching of bridging carbonate species. In addition to these bands, we also observed a weak band at 2513 cm^{-1} which was due to the linearly adsorbed CO_2 at cation site. On 60%CaO/Al_2O_3 catalyst, bicarbonate species dominated and there was no bidentate or unidentate carbonate species. These indicated that 60%CaO/Al_2O_3 catalyst had basic sites having a different chemical environment, represented by dominated bicarbonate species, than those found on pure CaO, which led to different basic strengths. Indeed, the absorption wavenumber of the strongest band on pure CaO occurred at a center wavenumber of 1454 cm^{-1} with the splitting located at 1424 and 1484 cm^{-1} whereas on 60%CaO/Al_2O_3 catalyst, the strongest band was seen at 1432 cm^{-1} without any band splitting. In other words, the absorption band found on 60%CaO/Al_2O_3 catalyst occurred at weaker absorption band energy than the band energy observed on pure CaO. Thus, the basic site strength on 60%CaO/Al_2O_3 catalyst as compared to that on pure CaO was weak. This indicated that the weak basic strength due to formation of

Table 1
XRD patterns and their corresponding crystalline phases with standard reference cards.

Observed Diffraction Angles in Fig. 1, which match with ones in standard reference card	Crystalline Phases	Standard Reference Card Number
18.03, 36.67, 47.09	$Ca(OH)_2$	00-044-1481
23.02, 29.41, 35.97, 39.40, 43.15, 47.12, 47.49, 48.51, 57.40, 60.68, 64.68	$CaCO_3$	00-005-0586
32.20, 37.34, 53.86, 67.38	CaO	00-037-1497
27.77, 29.70, 32.09, 36.54, 39.49, 46.51, 47.65, 53.85, 57.48, 67.20, 67.25	Al_2O_3	00-046-1215
33.20, 35.89, 37.38, 43.09, 57.71	$2CaO.Al_2O_3.8H_2O$	00-045-0564
22.97, 23.42, 32.97, 33.17, 34.06, 35.79, 36.69, 37.17, 43.05, 46.94, 47.22, 47.47, 48.35, 55.00, 57.19	$3CaO.Al_2O_3.3CaCO_3.3H_2O$	00-041-0215

Table 2
Total basicity (μmol CO_2/g of catalyst) using FTIR.

Catalysts calcined at 700 °C	Total Basicity (μmol CO_2/g of catalyst) using FTIR	FTIR CO_2 adsorption maximum wavenumber (1/cm)
60% CaO/Al_2O_3	41.0	1266
		1333
		1432
		1635
		1798
		2513
Pure CaO	192.6	1074
		1424
		1484
		1653
		1794
		2564
Pure Al_2O_3	47.1	1404
		1533
		1637

dominated bicarbonate species, observed on 60%CaO/Al_2O_3 catalyst, was the main reason for the high microalgal lipid conversion to the fatty acid ethyl esters biodiesel.

3.2. The effects of reaction conditions on the ethyl esters biodiesel yields

Fig. 2 compares the ethyl ester biodiesel yields obtained on the 60 wt% CaO/Al_2O_3 catalyst as a function of ethanol:lipid molar ratios, the catalyst amounts, and the reaction times at a constant reaction temperature of 50 °C. As seen in the figure, the biodiesel yield increased as the catalyst amount was increased from 6.0 wt% to 12 wt%, regardless of ethanol:lipid molar ratios and reaction times. For instance, biodiesel yield increased from ~59% to 74% under the ethanol:lipid molar ratio of 12 in 30 min of the reaction time as the catalyst amount was increased from 6 wt% to 12 wt%. In contrast, the biodiesel yield did not change as a function of the reaction time at 24 and 48 of the ethanol:lipid molar ratios when the catalyst amount was 12 wt% or 18 wt%. The biodiesel yield increased with the reaction time when the ethanol:lipid molar ratio was 12 and the catalyst amount was 6.0 wt% of the lipid amount. This increase of the biodiesel yield with the time was expected for a reversible reaction which was away from the equilibrium conversion but once the equilibrium was reached, the conversion should stay constant with increase of the reaction time. In addition, the increase of the ethanol:lipid molar ratio resulted in accelerated forward transesterification reaction rate; hence, higher biodiesel yields, which was similar to that observed with vegetable oil transesterification under excess methanol [12,21]. The ethanol:oil molar ratio used in this study was at least 4 times higher than the stoichiometric ethanol:oil molar ratio of 3. Thus, 100% of the equilibrium conversion could be expected at higher ethanol:lipid molar ratios. However, at 24 and 48 of ethanol:lipid molar ratios, biodiesel yields higher than 90%, obtained at 30 min, decreased when the reaction time was increased to 60 min and after that, it stayed constant at 120 min. As seen in Fig. 3, at 6 wt% of the catalyst amount and 24 of ethanol:lipid molar ratio, the biodiesel yield decreased from ~90% to ~71% as the reaction time increased from 30 min to 60 min and then, at 120 min of the reaction time, the yield stayed constant; thus, indicating that the equilibrium biodiesel yield was reached. Similarly, at 6 wt% of the catalyst amount and 48 of ethanol:lipid molar ratio, the biodiesel yield decreased from ~98% to ~79% as the reaction time was increased from 30 min to 60 min and then, the yield stayed constant at ~85% within ±4.8% of the experimental uncertainty of this study at 120 min. Decreasing and staying constant trend of the biodiesel yield with the reaction time, observed at 24 and 48 of ethanol:lipid molar ratios, could be due to the glycerolysis of lipids or oils as shown in equations (1)–(3) below, occurring in series with the transesterification reaction of the lipids/oils given in equations (4)–(6) below [32–34].

Glycerolysis of a triacylglyceride:

$$TAG + 2\ Gly \leftrightarrow 3\ MAG \quad (1)$$

$$TAG + Gly \leftrightarrow MAG + DAG \quad (2)$$

$$DAG + Gly \leftrightarrow 2\ MAG \quad (3)$$

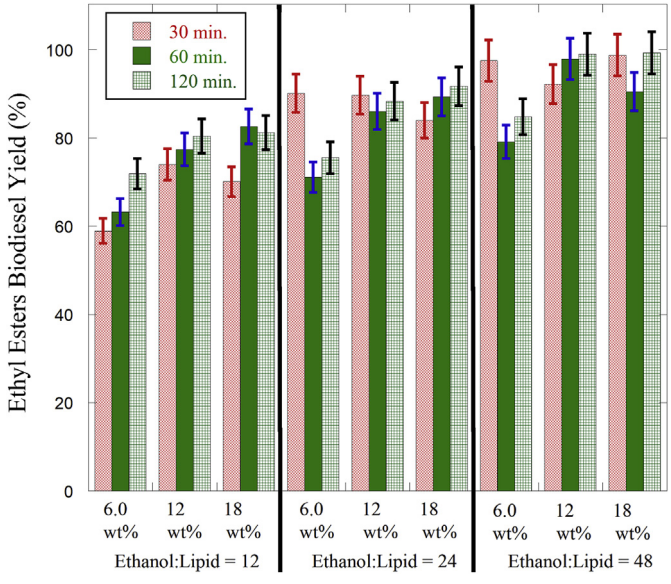

Fig. 2. Ethyl esters biodiesel yield as a function of ethanol:oil molar ratio, the catalyst amount and reaction time at 50 °C and 1.0 atm.

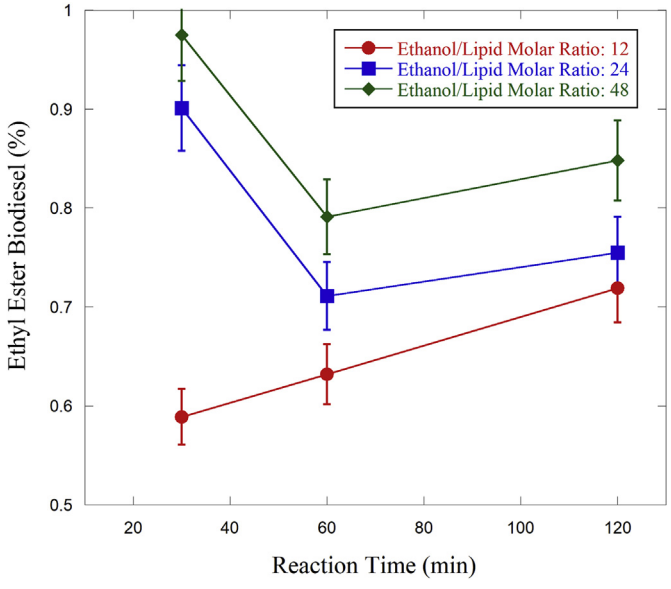

Fig. 3. Ethyl esters biodiesel yield as a function of ethanol:oil ratio and reaction time for a constant catalyst amount, 6 wt% of the microlipid, at 50 °C and 1.0 atm.

Table 3
The transesterification of *N. oculata* to fatty acid ethyl esters biodiesel.

Catalyst amount wt% of lipid	Ethanol:Lipid (mol:mol)	Reaction Time (min.)	Biodiesel Yield (%)
6	24	30	82.1
12	24	30	96.2
12	12	120	62.0
12	24	120	95.5
12	48	120	99.0

Transesterification of a triacylglyceride:

$$TAG + EtOH \leftarrow\rightarrow FAEE + DAG \quad (4)$$

$$DAG + EtOH \leftarrow\rightarrow FAEE + MAG \quad (5)$$

$$MAG + EtOH \leftarrow\rightarrow FAEE + Gly \quad (6)$$

where TAG was triacylglyceride; MAG was monoacylglyceride; DAG was diacylglyceride; Gly was glycerol; FAEE was fatty acid ethyl ester and EtOH was ethanol.

Zhong et al. [34] showed the effects of the solvent type, the catalyst type/amounts on the glycerolysis of oils at various temperatures. They found that the glycerolysis conversion increased with the increased solvent amount at various temperatures. Similarly, Kore et al. [35] reported that the glycerolysis of oils proceeded faster in the presence of a base catalyst. Our findings shown in Fig. 3 could be explained in such away that the conversion of microalgal lipid to the fatty acid ethyl esters (FAEE) in 30 min of the reaction time was found to be already higher than 90% which meant that there was enough glycerol formed through the reactions 4–6. Thus, glycerolysis of triacylglyceride occurred through the reactions 1, 2 or 3 as the reaction time increased to 60 min. As a result, the reverse reaction of the reactions 4 and 5 consumed FAEE; thus, leading to the decreased biodiesel yield (i.e. decreased triacylglyceride conversion), which was observed at 60 min. Unfortunately, TAG, MAG, DAG and Gly could not be measured using the GC-column in this study, Thus, the reactions suggested in equations (1)–(3) was confirmed by measuring FAEE formation as a function of reaction time, as seen in Fig. 3.

We also studied the transesterification of *N. oculata* to ethyl esters biodiesel under selected ethanol:lipid molar ratios, the reaction times and the amount of the catalyst, that were found to produce high biodiesel yields. The main reasons of choosing selected reaction conditions were twofold: 1) they have similar fatty acid compositions; 2) local supply of *N. oculata* microalgal paste was unfortunately limited. As seen in Table 3, ethyl esters biodiesel yield increased from ~82% to ~96% in 30 min of the reaction time at ethanol:lipid molar ratio of 24 when the catalyst amount was increased from 6.0 wt% to 12 wt% at 50 °C. Also, the biodiesel yield increased from ~62% to ~99% at 12 wt% of the catalyst amount and 120 min of the reaction time as ethanol:lipid molar ratio was increased from 12 to 48. This was the same trend as we observed using *Spriluna sp.* in this study. This was plausible because *Spriluna sp.* and *N. oculata* had similar compositions of fatty acids. Similarly, we found that pure CaO and pure Al_2O_3 catalysts were not active in the production of ethyl esters biodiesel from *N. oculata* microalgal lipid at any ethanol:lipid molar ratio and any catalyst amount at 50 °C. In fact, these findings are in parallel with our previous study on the transesterification of *N. oculata* microalgal lipid using methanol at 50 °C [12].

The ethyl ester biodiesel, produced in this study, contained less than 12 ppm of the dissolved Ca cations, which was determined using ICP-MS. This was much lower than the amount of Ca cation, which was 500 ppm, found in the methyl ester biodiesel in our previous study [21]. Besides, we checked if 12 ppm Ca ions could contribute to the homogeneous transesterification of the algal lipid with ethanol at 50 °C and found that the ethyl ester formation was zero within the experimental uncertainty of this study.

4. Conclusions

90–99% ethyl esters biodiesel was produced from microalgae *N. oculata* and *Spirulina sp.* lipids over 60%CaO/Al_2O_3 under 24 and 48 of ethanol:lipid molar ratios in 30 min at 50 °C and 1.0 atm whereas no biodiesel was produced over commercial pure CaO, $CaCO_3$ and $Ca(OH)_2$ catalysts and also pure Al_2O_3 under the same reaction conditions. Basic strength of 60%CaO/Al_2O_3 was weaker than those of pure commercial calcium oxides and pure Al_2O_3 catalysts even though pure catalysts had higher basicity. At high ethanol:lipid molar ratios and 60 min, glycerolysis of triacylglyceride occurred in series with the reverse of the transesterification of the triacylglyceride.

Declarations of interest

None.

Acknowledgements

Authors would like to greatly thank Prof. Dr. Durmus Yilmaz of Ege University for the microalgal lipid paste and also, to thank Dr. Emin Selahattin Umdu for the analysis of calcium ions in biodiesel using ICP-MS.

This research did not receive any specific grant from funding agencies in the public, commercial, or not-for-profit sectors.

Appendix A. Supplementary data

Supplementary data to this article can be found online at https://doi.org/10.1016/j.renene.2019.06.093.

References

[1] J.J. Baruch, Combating global warming while enhancing the future, Technol. Soc. 30 (2008) 111–121.
[2] U.S. Energy Information Administration, Annual Energy Outlook 2018 with Projections to 2050, U.S. Department of Energy, Washington, 2018.
[3] T. Zachariadis, N. Kouvaritakis, Long-term outlook of energy use and CO_2 emissions from transport in Central and Eastern Europe, Energy Policy 31 (2003) 759–773.
[4] Y. Chisti, Biodiesel from microalgae beats bioethanol, Trends Biotechnol. 26 (2008) 126–131.
[5] B.E. Rittmann, Opportunities for renewable bioenergy using microorganisms, Biotechnol. Bioeng. 100 (2008) 203–212.
[6] Y. Chisti, Biodiesel from microalgae, Biotechnol. Adv. 25 (2007) 294–306.
[7] S.N. Naik, L.C. Meher, D.V. Sagar, Technical aspects of biodiesel production by transesterification – a review, Renew. Sustain. Energy Rev. 10 (2006) 248–268.
[8] P.M. Schenk, S.R. Thomas-Hall, E. Stephens, U.C. Marx, J.H. Mussgnug, C. Posten, O. Kruse, B. Hankamer, Second generation biofuels: high-efficiency microalgae for biodiesel production, Bioenergy Res. 1 (2008) 20–43.
[9] X. Miao, Q. Wu, Biodiesel production from heterotrophic microalgal oil, Bioresour. Technol. 97 (2006) 841–846.
[10] X. Li, H. Xu, Q. Wu, Large-scale biodiesel production from microalga *Chlorella*

protothecoides through heterotrophic cultivation in bioreactors, Biotechnol. Bioeng. 98 (2007) 764–771.
[11] A.B.M.S. Hossain, A. Salleh, A.N. Boyce, P. Chowdhury, M. Naqiuddin, Biodiesel fuel production from algae as renewable energy, Am. J. Biochem. Biotechnol. 4 (2008) 250–254.
[12] E.S. Umdu, M. Tuncer, E. Seker, Transesterification of *Nannochloropsis oculata* microalga's lipid to biodiesel on Al_2O_3 supported CaO and MgO catalysts, Bioresour. Technol. 100 (2009) 2828–2831.
[13] A. Carrero, G. Vicente, R. Rodríguez, M. Linares, G.L. del Peso, Hierarchical zeolites as catalysts for biodiesel production from Nannochloropsis microalga oil, Catal. Today 167 (2011) 148–153.
[14] S.H. Teo, A. Islam, T. Yusaf, Y.H. Taufiq-Yap, Transesterification of *Nannochloropsis oculata* microalga's oil to biodiesel using calcium methoxide catalyst, Energy 78 (2014) 63–71.
[15] A. Carrero, G. Vicente, R. Rodriguez, G.L. del Peso, C. Santos, Synthesis of fatty acids methyl esters (FAMEs) from *Nannochloropsis gaditana* microalga using heterogeneous acid catalysts, Biochem. Eng. J. 97 (2015) 119–124.
[16] A. Guldhe, C.V.R. Moura, P. Singh, I. Rawat, E.M. Moura, Y. Sharma, F. Bux, Conversion of microalgal lipids to biodiesel using chromium-aluminum mixed oxide as a heterogeneous solid acid catalyst, Renew. Energy 105 (2017) 175–182.
[17] P.A. Leggieri, M. Senra, L. Soh, Cloud point and crystallization in fatty acid ethyl ester biodiesel mixtures with and without additives, Fuel 222 (2018) 243–249.
[18] O.J. Alamu, M.A. Waheed, S.O. Jekayinfa, Effect of ethanol-palm kernel oil ratio on alkali-catalyzed biodiesel yield, Fuel 87 (2008) 1529–1533.
[19] M.K. Lam, K.T. Lee, Mixed methanol-ethanol technology to produce greener biodiesel from waste cooking oil: a breakthrough for SO_4^{2-}/SnO_2-SiO_2 catalyst, Fuel Process. Technol. 92 (2011) 1639–1645.
[20] E. Li, Z.P. Xu, V. Rudolph, MgCoAl–LDH derived heterogeneous catalysts for the ethanol transesterification of canola oil to biodiesel, Appl. Catal. B Environ. 88 (2009) 42–49.
[21] E.S. Umdu, Methyl Ester Production from Vegetable Oils on Heterogeneous Basic Catalysts, Izmir Institute of Technology, Izmir, 2008.
[22] E. Yalman, Biodiesel Production from Safflower Using Heterogeneous CaO Based Catalysts, Izmir Institute of Technology, Izmir, 2012.
[23] Y. Durmaz, Vitamin E (α-tocopherol) production by the marine microalgae *Nannochloropsis oculata (Eustigmatophyceae)* in nitrogen limitation, Aquacult 272 (2007) 717–722.
[24] A. Hara, N.S. Radin, Lipid extraction of tissues with a low-toxicity solvent, Anal. Biochem. 90 (1978) 420–426.
[25] S. Fredriksson, K. Elwinger, J. Pickova, Fatty acid and carotenoid composition of egg yolk as an effect of microalgae addition to feed formula for laying hens, Food Chem. 99 (2006) 530–537.
[26] A. Roncarati, A. Meluzzi, S. Acciarri, N. Tallarico, P. Melotti, Fatty acid composition of different microalgae strains (*Nannochloropsis* sp., *Nannochloropsis oculata* (Droop) Hibberd, *Nannochloris atomus* Butcher and *Isochrysis* sp.) according to the culture phase and the carbon dioxide concentration, J. World Aquac. Soc. 35 (2004) 401–411.
[27] B.D. Cullity, Elements of X-Ray Diffraction, second ed., Addison-Wesley, Massachusetts, 1978.
[28] K. Tanabe, M. Misono, Y. Ono, H. Hattori, New Solid Acids and Bases Their Catalytic Properties, Elsevier, Amsterdam, 1989.
[29] JCPDS-ICDD, PDF-2 Database International Centre for Diffraction Data, 2000. Pennsylvania.
[30] P. Gruene, A.G. Belova, T.M. Yegulalp, R.J. Farrauto, M.J. Castaldi, Dispersed calcium oxide as a reversible and efficient CO_2-sorbent at intermediate temperatures, Ind. Eng. Chem. Res. 50 (2011) 4042–4049.
[31] M.I. Zaki, H. Knozinger, B. Tesche, G.A.H. Mekhemer, Influence of phosphonation and phosphation on surface acid–base and morphological properties of CaO as investigated by in situ FTIR spectroscopy and electron microscopy, J. Colloid Interface Sci. 303 (2006) 9–17.
[32] H. Noureddini, V. Medikonduru, Glycerolysis of fats and methyl esters, JAOCS (J. Am. Oil Chem. Soc.) 74 (1997) 419–425.
[33] N. Zhong, L. Li, X. Xu, L.Z. Cheong, X. Zhao, B. Li, Production of diacylglycerols through low-temperature chemical glycerolysis, Food Chem. 122 (2010) 228–232.
[34] N. Zhong, L. Li, X. Xu, L.Z. Cheong, Z. Xu, B. Li, High yield of monoacylglycerols production through low-temperature chemical and enzymatic glycerolysis, Eur. J. Lipid Sci. Technol. 115 (2013) 684–690.
[35] P.P. Kore, S.D. Kachare, S.S. Kshirsagar, R.J. Oswal, Base catalyzed glycerolysis of ethyl acetate, Org. Chem. Curr. Res. 1 (2012) 108–111.